Modification of Spectrin in Red Cell Membranes by the Lipid Peroxidation Product 4-Hydroxy-2-nonenal Associated with the Changes in Red Cell Membrane Properties

（赤血球膜スペクトリンの脂質過酸化産物 4-ヒドロキシ-2-ノネナールによる分子修飾と赤血球膜物性の変化）

Nobuto Arashiki

Laboratory of Molecular Medicine, Department of Veterinary Clinical Sciences, Graduate School of Veterinary Medicine, Hokkaido University

Contents

Abbreviations

Abbreviations used in this study are as follows:

HNE	4-hydroxy-2-nonenal
IOV	inside-out vesicle
MALDI-TOF MS....	matrix-assisted laser desorption/ionization time-of-flight mass spectrometry
MgATP	adenosine 5'-triphosphate, magnesium salt
PBS	phosphate-buffered saline
PVP	polyvinylpyrrolidone
RBC	red blood cell
SDS-PAGE	sodium dodecylsulfate-polyacrylamide gel electrophoresis
t-BOOH	*tert*-butylhydroperoxide

In the present study, one-letter and three-letter abbreviations for amino acid residues are employed.

Preface

Oxidative stress is associated with various pathological conditions, including inflammation, diabetes, neurodegenerative diseases, and hemolytic anemia with various degrees. The potential for red blood cells (RBCs) to undergo autooxidative destruction is great because the cell is loaded with about 20 mM hemoglobin, most of which is bound to oxygen and can release a highly reactive superoxide ion, leaving behind it methemoglobin. Continued oxidation of methemoglobin leads to generation of irreversibly oxidized hemichromes, to precipitation, and eventually to the formation of Heinz bodies. Hemichromes and Heinz bodies can destroy functions of RBC membranes directly or can cause oxidation of membrane components. These may include lipid peroxidation and protein cross-linking, resulting in formation of RBCs that are rigid and are susceptible to trapping in sinusoidal structures. Consequently, the extravascular and intravascular destructions of such RBCs occur.

The mechanical properties of RBC membranes, i.e., membrane stability and deformability, are primarily attributed to the functions of membrane skeletal proteins that underlie the cytoplasmic surface of the lipid bilayer. Therefore, these membrane proteins are likely to be the targets of the oxidative attacks. In addition, the local generation and accumulation of peroxidation products in the membrane, by affecting membrane protein function, might be involved in senescence of RBCs under physiological conditions. However, no substantial study has been reported in RBCs except for a few studies on the adduct formation between spectrin and denatured globin and the association of band 3 with Heinz bodies.

The purpose of the present study was to examine the presence and significance of the covalent modification of membrane skeletal proteins by lipid peroxidation products in RBCs. The present study demonstrates that protein modification with a lipid peroxidation end product, 4-hydroxy-2-nonenal occurs preferentially in spectrin at the interface between the skeletal proteins and lipid bilayer. The data also show that this reaction is associated with reduction in membrane mechanical properties of RBCs.

This study has been published in part as follows:

1) Arashiki, N., Otsuka, Y., Ito, D., Yang, M., Komatsu, T., Sato, K., and Inaba, M. (2010) The covalent modification of spectrin in red cell membranes by the lipid peroxidation product 4-hydroxy-2-nonenal. *Biochem. Biophys. Res. Commun.* **391**, 1543-1547.

Introduction

Spectrin, a major constituent of the human RBC membrane skeleton, acts as a scaffolding protein and mediates the organization and assembly of a diverse set of proteins in specialized membrane domains (Bennett and Healy, 2008). Spectrin is a flexible, rod-like protein formed by two end-to-end associated heterodimers composed of α and β subunits, with sizes of 280 kDa and 246 kDa, respectively. In RBCs, the spectrin-actin network is linked to the lipid bilayer through protein-protein interactions, specifically spectrin-protein 4.1R-glycophorin C and spectrin-ankyrin-band 3 associations, and through direct association of spectrin with phosphatidylserine (PS) in the inner bilayer leaflet (Cohen *et al*., 1986; Manno *et al*., 2002; Mohandas and Gallagher, 2008). Such vertical interactions between the spectrin-actin skeleton and lipid bilayer play pivotal roles in maintaining RBC membrane stability (Manno *et al*., 2002; Low *et al*., 1991; Inaba *et al*., 1996). Spectrin loss reduces the membrane mechanical resilience, leading to spherocyte formation in various types of hereditary spherocytosis (Tse and Lux, 2001; Mohandas and Gallagher, 2008; Perrotta *et al*., 2008). In contrast with its role in congenital disorders, less is known about acquired spectrin damage. Previous studies have focused on the oxidation of spectrin sulfhydryl groups, revealing that RBC exposure to oxidative conditions causes morphological and mechanistic changes, principally through spectrin oxidation (Snyder *et al*., 1998; Wagner *et al*., 1987). Furthermore, mild oxidation reportedly causes functional and structural changes, leading to the reduced interaction of spectrin with protein 4.1 (Becker *et al*., 1986).

In contrast, membrane phospholipid peroxidation, that is proceeded by a free radical

chain reaction mechanism (Yang *et al*., 2003), generates various cytotoxic aldehydes and alkenals that can damage proteins and other cellular constituents (Esterbauer *et al*., 1991; Schneider *et al*., 2001; Uchida, 2003). 4-Hydroxy-2-nonenal (HNE) is the most abundant and toxic aldehyde generated by the oxidation of plasma membrane polyunsaturated fatty acids, such as arachidonic acid. HNE is fairly stable and present in relatively higher amounts in biological membranes under the conditions of oxidative stress (Esterbauer *et al*., 1991). HNE is a highly reactive electrophile that reacts with the side chains of various amino acid residues, including Cys, His, and Lys, to form Michael-type adducts and Schiff-base adducts of HNE-Lys (Fig. 1A) (Esterbauer *et al*., 1991; Liu *et al*., 2003; Peterson and Doorn, 2004). Protein modification by HNE causes serious detrimental effects in the cell, due to the resulting functional defects and cross-linking of proteins (Fig. 1B) (Uchida *et al*., 1993; Montine *et al*., 1996; Lauderback *et al*., 2001; Murray *et al*., 2007; Stewart *et al*., 2007; Kokubo *et al*., 2008). HNE also accumulates in RBCs (Ando *et al*., 1995), leading to the covalent modification of membrane proteins (Uchida *et al*., 1997). However, the target proteins for HNE modification remain unknown.

These findings have suggested that oxidative environments under physiological or disease conditions may cause spectrin modifications by HNE, leading to deleterious changes in the plasma membrane mechanical properties. The purpose of the present study was to examine the presence and significance of covalent spectrin modifications by HNE in RBCs. The present study was focused on membrane proteins in human RBCs since their structures and the roles in the mechanical properties of the RBC membrane have been well documented (Tse and Lux, 2001; Mohandas and Gallagher, 2008). We used anti-HNE antibodies and

matrix-assisted laser desorption/ionization time-of-flight mass spectrometry (MALDI-TOF MS) to identify HNE-modified proteins in RBC membranes, and found that spectrin was the primary target of HNE. Then, the effects of HNE modification on the RBC membrane mechanical properties were characterized by some biophysical and biochemical approaches.

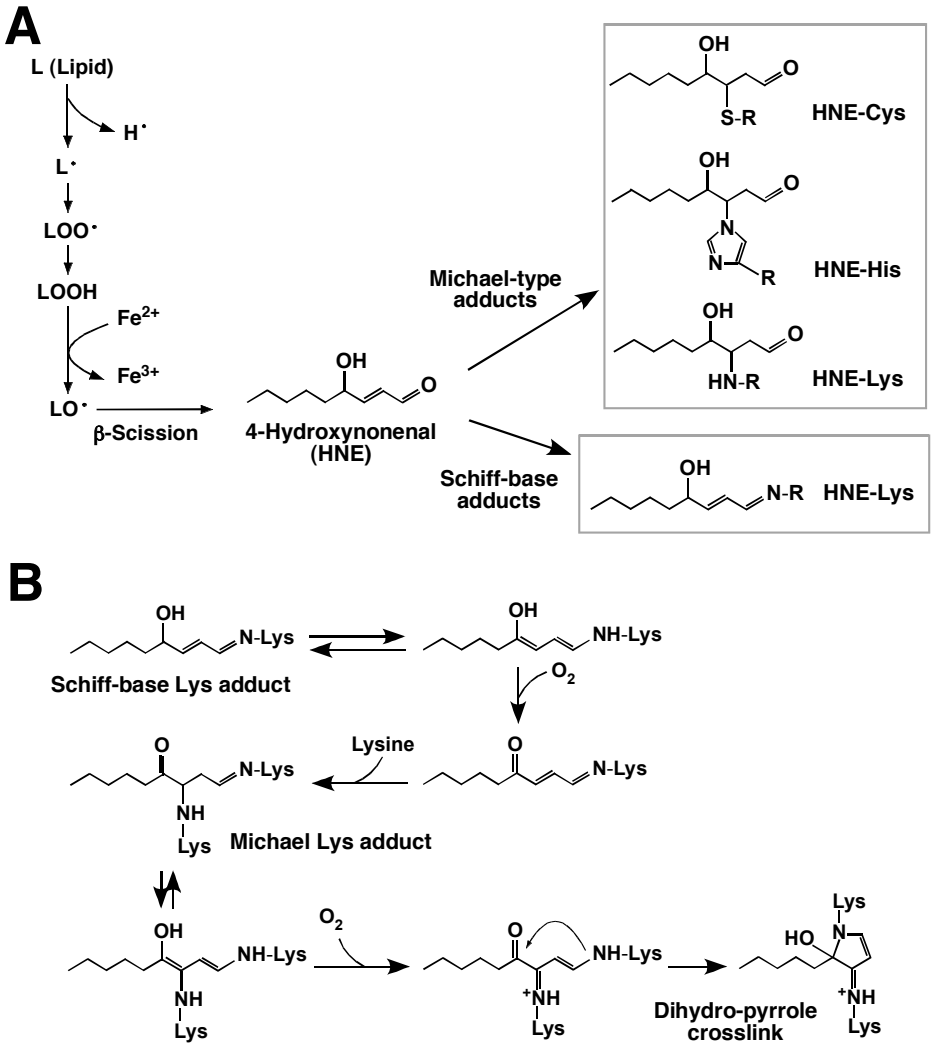

Figure 1. Lipid peroxidation, formation of HNE-amino acid adducts, and protein crosslinking.

A. A chain reaction of lipid (*L*) peroxidation generates lipid peroxides. Lipid peroxides undergo spontaneous decomposition yielding a number of aldehydes including HNE. HNE can react with Cys, His, and Lys in proteins, forming Michael adducts or Schiff-base adducts (only with Lys). B. The reaction of HNE with proteins is frequently associated with their covalent crosslinking leading to the formation of fluorophores such as a Lys-derived dihydro-pyrrole derivative. Reproduced from Yang *et al*. (2003) and Liu *et al*. (2003) with several changes.

Materials and Methods

Preparation of RBC membrane ghosts and spectrin-actin extracts

After obtaining informed consent, blood was obtained from healthy volunteers. Blood was also obtained from dogs, cats, and cattle housed at the Graduate School of Veterinary Medicine, Hokkaido University. All experimental procedures met with the approval of the Laboratory Animal Experimentation Committee, Graduate School of Veterinary Medicine, Hokkaido University.

Preparation of RBC membrane ghosts and extraction of spectrin heterodimers ($\alpha\beta$) with a hypotonic buffer were performed as described previously (Inaba *et al*., 1996). In some experiments, RBC ghosts were prepared by hemolysis in hypotonic buffer (5 mM Tris/Cl [pH 7.4], 5 mM KCl, and 1 mM $MgCl_2$) with or without 0.6 mM MgATP (Sigma), as described previously (Manno *et al*., 2002). We also obtained ghosts from RBCs separated into different fractions using a discontinuous arabinogalactan gradient (Tiffert *et al*., 2005).

SDS-PAGE and immunoblotting

Membrane proteins were separated by SDS-PAGE on 6.5% or 10% SDS-gels followed by staining with Coomassie brilliant blue or immunoblotting. Immunoblotting was performed as described previously (Ito *et al*., 2006) using antibodies against HNE-Michael adducts (Calbiochem), HNE-His (monoclonal antibody HNEJ-2; Nikken SEIL Co., Fukuroi, Japan), and canine spectrin (Inaba *et al*., 1996). One-dimensional spectrin peptide mapping was performed as described previously (Inaba and Maede, 1989; Inaba *et al*., 1992) using V8

protease (Sigma).

MALDI-TOF MS analysis of spectrins.

After separation by SDS-PAGE, proteins in the gel slices were reduced with $NaBH_4$ for 30 minutes at an ambient temperature unless otherwise indicated. This was done to detect unstable reversibly formed adducts, such as HNE-Lys Michael adducts (Fenaille *et al*., 2003). The proteins were subsequently stained with Coomassie brilliant blue and digested in gel slices with 10 μg/ml of trypsin Gold (Promega) for 16 hours at 37ºC. Prior to protease digestion, the Cys residues were reduced with 10 mM dithiothreitol and alkylated with 55 mM iodoacetamide. Peptides were eluted from gels, desalted using C18 ZipTips (Millipore), and crystallized using saturated α-cyano-4-hydroxy-cinnamic acid (Bruker Daltonics) as a matrix. Full-scan mass spectra of the tryptic peptides from 800-3,000 *m/z* were collected in positive mode by averaging 100-250 spectra using a Bruker autoflex MALDI-TOF mass spectrometer. Measured peptide masses were used to search the NCBI and Swiss-Prot sequence database for protein identification using MASCOT software (Matrix Science).

In vitro formation of HNE-protein adducts in red cells and red cell ghosts

A packed 10% cellular volume of RBCs was suspended in phosphate-buffered saline (PBS) containing 5 mM glucose. After incubation for various times (0-6 hours) at 37ºC in the presence or absence of 0.1-1.0 mM HNE (Calbiochem), the cells were washed with PBS. Membrane ghosts were then prepared as described above. Ghost proteins were labeled with HNE by incubating PBS-suspended ghosts (1 mg protein/ml) with 0.01-1.0 mM HNE at 37ºC

for appropriate time periods (0-60 minutes), followed by SDS-PAGE and immunoblotting. In some experiments, incubation was performed in hypotonic buffer with 0.1 mM MgATP.

In vitro oxidation of RBCs with *tert*-butylhydroperoxide and analysis of spectrin

RBCs suspended in PBS containing 5 mM glucose were incubated at 37ºC for the time periods indicated in the presence of 0.3 or 3.0 mM *tert*-butylhydroperoxide (*t*-BOOH, Wako Pure Chemical Industries, Tokyo, Japan). After incubation, RBCs were collected by centrifugation and directly dissolved in SDS-PAGE sample buffer. An SDS-PAGE was performed, followed by immunoblotting to detect the HNE-spectrin adducts.

Measurement of red cell membrane mechanical properties

After incubation in the presence or absence of HNE, as described above, RBCs were washed with PBS, suspended in 3.5% polyvinylpyrrolidone (PVP, Sigma) at 30 μl of packed red cells/4 ml of PVP solution, and exposed to an increasing shear stress (0-150 dynes/cm^2) in the ektacytometer as described previously (Chasis and Mohandas, 1986). Deformability index (DI) versus applied shear stress curve was analyzed to quantitate membrane deformability.

Measurement of binding of spectrin to the inside-out vesicles

The RBC ghosts were extracted for spectrin as described above. The resultant inside-out vesicles (IOVs) were resealed by incubating in PBS at 37ºC for 40 minutes. Extracted spectrin heterodimers (0-150 μg) were incubated in PBS in the presence or in the absence of 0.1 mM HNE at 37ºC for the appropriate time. To this were added IOVs

containing 10 μg of proteins and incubated on ice for 90 minutes. The reactions were applied on 8% sucrose in PBS followed by centrifugation at 33,500 x g for 50 minutes at 4ºC to obtain spectrin bound to the IOVs. The contents of α- and β-spectrin were analyzed by SDS-PAGE and normalized with the amount of band 3 in the IOVs by densitometric scanning of the Coomassie blue-stained gels.

Statistical analysis

Paired Student's *t*-test was used to assess statistical significance.

Results

I. Characterization of HNE modification of RBC α- and β-spectrin

HNE modification of α- and β-spectrin in human RBC membranes

Immunoblotting analysis revealed the presence of polypeptides that had reacted with the anti-HNE antibody. These polypeptides were located at positions corresponding to α- and β-spectrin in the freshly prepared human RBC membranes and in the crude spectrin-actin preparation extracted from the ghosts (Fig. 2A). These signals were weak and required > 15 seconds for detection when 5 ~ 10 μg of membrane proteins were loaded. Spectrin, especially β-spectrin, also reacted with the anti-HNE-His adducts, suggestive of a predominance of HNE-His adducts in β-spectrin (Fig. 2A). When limited digestion of β-spectrin with V8 protease was performed, more than 20 polypeptides with sizes of < 50 kDa were detected by Coomassie blue staining. Among these, only the 45- and 40-kDa fragments strongly reacted with the anti-HNE antibodies (Fig. 2B).

The spectrin polypeptides were analyzed to determine the positions where these spontaneous modification with HNE occurred in spectrins from freshly prepared RBC ghosts. MALDI-TOF MS detected 50 ~ 70 tryptic peptides that covered ~ 25-35% of the total amino acid residues of α- and β-spectrin. Several independent analyses consistently showed that a dozen or more distinct peptides derived from either α- and β-spectrin contained one or more Michael-type HNE-amino acid adduct and Schiff base conjugate (Table 1 and Fig. 3). For example, in β-spectrin reduced with $NaBH_4$, the MALDI-TOF MS consistently detected an

HNE-modified species at 2,622.4 *m/z* for the peptides I<u>HC</u>LENVD<u>K</u>ALQFL<u>K</u>EQR (amino acid residues 110-127) derived from the N-terminal actin-binding domain of this subunit. The observed mass shift of 438 *m/z* (= 158 + 2 × 140 *m/z*) was indicative of a Michael addition reaction with mass shifts of 158 *m/z* at either the 2nd or 3rd underlined His or Cys residue, respectively. The mass shift of 438 *m/z* was also indicative of Schiff base adducts with mass shifts of 280 *m/z* (= 2 × 140 *m/z*) at the two underlined Lys residues. This is because reduction with $NaBH_4$ increases the characteristic mass shifts of 156 and 138 *m/z* for Michael and Schiff base adducts, respectively, by 2 atomic mass units (Fenaille *et al*., 2003). When β-spectrin was analyzed without reduction, peaks at 1,382.6 and 2,239.2 *m/z*, shifted by 312 (= 2 × 156) and 468 (= 3 × 156) atomic mass units, respectively, were detected for the corresponding peptides I<u>HC</u>LENVDK and I<u>HC</u>LENVD<u>K</u>ALQFLK, suggesting that all underlined residues could form Michael-type HNE adducts. Together with the data for the mass shifts of several other peptides (Table 1), these results allow us to predict that all Cys-, His-, and Lys-Michael adducts and Schiff base Lys adducts are present in both α- and β-spectrin, consistent with our immunoblot results with anti-HNE antibodies.

Fig. 3 illustrates the positions and types of HNE adduct formation obtained by MALDI-TOF MS for α- and β-spectrin. The presence of many HNE-amino acid adducts in the β-spectrin N-terminal region is compatible with the reactivity of the 45- and 40-kDa proteolytic fragments in immunoblotting shown in Fig. 2B. Subsequent MALDI-TOF MS analysis revealed that these proteolytic fragments were derived from the N-terminal domain and the first triple helical structural repeat, and that they contained peptides such as IHCLENVDK displaying $[M + H]^+$ with an *m/z* of 1,382.6, as described above.

Spectrins are the major targets of the lipid peroxidation product HNE in human RBC membranes

To further characterize HNE-spectrin adduct formation, we analyzed the covalent modification of spectrin in RBCs incubated with extrinsic HNE. Membrane ghosts treated with 0.1 mM HNE exhibited a marked increase in HNE-spectrin adduct contents within 10 minutes of incubation (Fig. 4A). Incubation also caused HNE labeling of several other membrane proteins with apparent sizes of 115, 110, 100, 80, and 43 kDa (Fig. 4A). These polypeptides were likely α- and β-adducin, band 3, protein 4.1R, and actin, respectively, judging from their migrating positions and antibody reactivities (data not shown). In contrast, when intact RBCs were incubated with HNE for several hours, a remarkable increase in the signals of HNE-protein adducts was found for spectrin, especially β-spectrin, but not for other membrane proteins (Fig. 4B).

Next, HNE-spectrin adduct formation was examined in RBCs exposed to the well-known oxidant *t*-BOOH. Incubation with 0.3 mM *t*-BOOH for 1 hour increased the HNE modification of spectrin, while decreasing the spectrin content of the human RBC membranes (Fig. 4C). As observed in RBCs incubated with extrinsic HNE (Fig. 4B), HNE signals were predominantly found in spectrins and were more prominent in β- than in α-spectrin. HNE adduct signals were also detected at the position corresponding to globins (~ 15 kDa), since RBCs were directly subjected to SDS-PAGE after incubation. While no obvious increase in HNE-spectrin adducts was demonstrated during incubation, the signal intensity of HNE-spectrin relative to that of spectrin (relative abundance of HNE-spectrin) increased

significantly due to the reduction in spectrin contents. Increasing the *t*-BOOH concentration to 3 mM caused striking decreases in α- and β-spectrin contents and the formation of high molecular weight species reactive to both the anti-HNE adducts and anti-spectrin antibodies within 2 hours of incubation (Fig. 4C). This indicates that the HNE-modified spectrin accumulated and formed irreversible aggregates in RBCs exposed to *t*-BOOH.

These results demonstrate that both extrinsic circulating HNE and intrinsic HNE, generated presumably through membrane lipid peroxidation, selectively react with spectrin at the protein-lipid bilayer interface. The data also suggest that the association status of spectrin with membrane lipids was different in intact RBCs and in the isolated membrane ghosts, so as to cause distinct patterns in HNE adduct formation for α- and β-spectrin.

Spectrin modification with HNE in RBC membranes from several animal species

To assess if HNE modification occurs, in general, in spectrins from various animals, membrane proteins in bovine, canine, and feline RBC membranes were analyzed for their HNE-protein adducts by immunoblotting. Membranes from these animals showed protein compositions that were principally the same with protein constituents in human RBCs so far judged by Coomassie brilliant blue staining (Fig. 5A) as reported previously (Inaba and Maede, 1988). However, there was a remarkable difference in HNE-modified proteins and their contents. In bovine and feline RBC membranes, HNE-spectrin adducts (α and β) was observed, but the their signal intensities were much less than that in human RBCs (Fig. 5B). Moreover, canine RBC spectrin showed no signals of HNE-protein adducts, indicating no

substantial and spontaneous formation of HNE-spectrin under physiological conditions. Instead, strong signals of HNE adducts were found in other polypeptides including a 95-kDa unknown polypeptide and protein 4.2. The abundant signals in protein 4.2 were also observed in feline RBC ghosts.

On the other hand, exposure to 0.1 mM HNE caused generation of HNE-protein adducts with profound signals in membranes from these animals; α- and β-spectrin were modified with HNE in all species, while HNE adducts appeared in the positions corresponding to band 3 and protein 4.1 in bovine RBC membranes, and protein 4.2 in canine and feline RBC membranes, respectively (Fig. 5C). Unidentified polypeptides of 200 kDa in bovine and 95 kDa in canine membranes also represented abundant HNE-protein adduct signals. These results demonstrated that the RBC membrane proteins accessible to HNE modification differ among species. Nonetheless, spectin appeared to be one of the major targets for HNE-adduct formation as in human RBC membranes as described above.

Effect of spectrin-lipid association on HNE modification of α- and β-spectrin

Therefore, we next compared spectrin labeling with HNE in membrane ghosts possessing different association status of spectrin with membrane lipids, i.e., ghosts prepared in the presence (MgATP ghost) or absence (control ghost) of MgATP (Manno *et al*., 2002). When ghosts were incubated with increasing HNE concentrations, we observed marked increases in the intensities of HNE-spectrin adducts in both MgATP and control ghosts (Fig. 6). In principle, when membrane proteins containing equivalent amounts of spectrins were exposed to HNE, spectrin labeling with HNE in the MgATP ghost was less abundant than in

the control ghost, and was much less than that in the crude spectrin-actin extract (Fig. 6A).

Remarkable differences between the MgATP and control ghosts were observed at lower HNE concentrations (0.05-0.3 mM). Immunoblotting revealed that the abundance of HNE signals relative to spectrin contents was significantly higher in the control than in the MgATP ghost (Figs. 6B and 6C), demonstrating that HNE spectrin labeling preferentially occurred in the control ghosts. In contrast, the MgATP ghost showed reductions in the spectrin contents and corresponding increases in high molecular weight aggregate formation, with prominent signals for both the anti-HNE adducts and anti-spectrin antibodies (Fig. 6B). These data suggest that HNE-modified spectrins in the MgATP ghosts tended to be cross-linked and aggregated, although the adduction levels were lower than those in control ghosts. Moreover, the HNE labeling of β-spectrin was nearly equivalent to that of α-spectrin in the MgATP ghost, whereas HNE labeling was predominantly found in α-spectrin in the control ghost, as observed in the crude spectrin-actin extract (Figs. 6A-6C).

II. The effects of HNE-spectrin adduct formation on the membrane properties of human RBCs

HNE-spectrin adducts in density-separated RBCs

Then, the contents of HNE-modified spectrin were analyzed for density-separated RBCs to examine if these adducts accumulate during RBC aging (Fig. 7). The lightest/youngest cell fraction showed HNE/spectrin ratios equivalent to those in fractions 3 and 4, which comprised ~90% of total cell counts (Fig. 7). No significant differences in the HNE levels of α- and β-spectrin were observed among fractions 1 through 4. The densest

fractions (fractions 5 and 6) had reduced HNE/spectrin ratios; an increase would have been expected if there was accumulation of HNE-spectrin adducts during RBC senescence. Similar results were obtained in three independent experiments, suggesting that human RBCs possess HNE-modified spectrin throughout their life-span with a slight reduction, rather than accumulation, in the levels of HNE-modified spectrins at senescence.

Effect of HNE modification of spectrin on RBC membrane mechanical properties

To determine the effect of HNE-spectrin adduct formation on mechanical properties of RBC membranes, we analyzed deformability, by ektacytometry, of RBCs in which spectrins were adducted with HNE by incubating the intact RBCs with HNE as described above (Fig. 4). RBCs exposed to 0.1 mM HNE exhibited reduction in the DI values to about 80% that of the control cells incubated in the absence of HNE, judging from the maximum DI values (DI_{max}) under shear stress at 150 dynes/cm^2 (Fig. 8). Difference in exposure periods, i.e., 1 hour or 4 hours, appeared to affect the initial phase of increasing the shear stress (0 ~ 40 dynes/cm^2), with less DI values in RBCs treated with 0.1 mM HNE for 4 hours. RBCs incubated for 1 hour with 1.0 mM HNE showed remarkably attenuated increase in DI in response to shear stress, and had a decreased DI_{max} value that was 60% that of the control cells. The DI_{max} value of HNE-treated cells exposed for 4 hours showed further reduction to only 40% of the control value. Since spectrin was the major target of HNE modification in the membrane under the condition employed (Fig. 4), the data obtained by ektacytometry analysis demonstrated that HNE modification of spectrin affected the mechanical properties, resulting

in reduced RBC membrane deformability.

Effect of HNE modification on binding of spectrin to the IOV

Spectrin bound to the IOVs in a concentration-dependent manner (Figs. 9A and 9B). The binding appeared to contain two phases with distinct dissociation constants (K_d) of 0.79 μM and 32 μM (Fig. 9C). Binding of HNE-spectrin to the IOVs exhibited a profile similar to that of the control spectrin, while it possessed K_d values of 0.41 μM and 40 μM, for high and low affinity phases, respectively (Figs. 9B and 9C), suggesting a slightly increased affinity of HNE-modified spectrin in binding to the IOVs in the high affinity component (Figs. 9B and 9C).

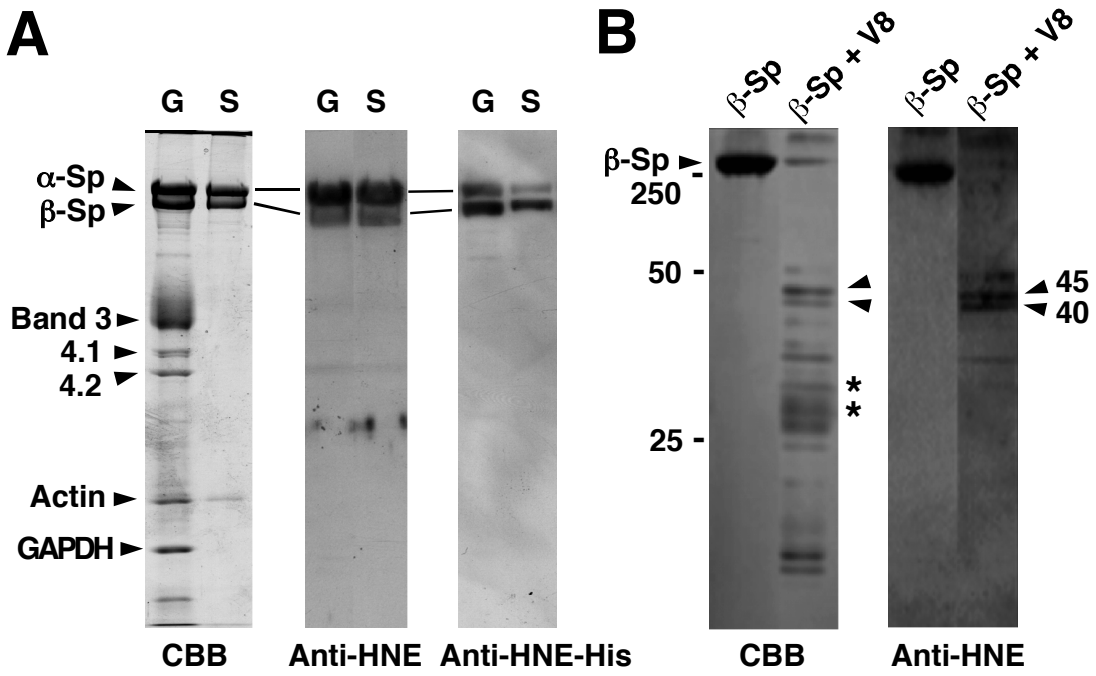

Figure 2. HNE-spectrin adducts in human RBC membranes.

A. Ghost membrane proteins (*G*, 8 μg/lane) and the crude spectrin/actin extracted from ghosts (*S*, 2-3 μg/lane) were separated on SDS-PAGE gels. Protein components were analyzed by Coomassie brilliant blue staining (*CBB*) and HNE-protein adduct formation was assessed by immunoblotting using anti-HNE (*Anti-HNE*) or anti-HNE-His (*Anti-HNE-His*) adduct antibodies. In immunoblotting, the membranes were exposed to the films for 1 minute. The migrating positions of the major membrane proteins, including α- and β-spectrin (*α-Sp* and *β-Sp*, respectively), are indicated. **B.** β-Spectrin separated on SDS-PAGE gels was sliced out and analyzed by one-dimensional peptide mapping in the presence (*β-Sp + V8*) or absence (*β-Sp*) of V8 protease, followed by *CBB* staining and immunoblotting with *Anti-HNE*. The 45- and 40-kDa proteolytic polypeptides exhibiting strong signals for HNE-protein adducts are indicated. The migrating positions of β-spectrin and of marker proteins (kDa) are also presented. Asterisks indicate polypeptides from V8 protease preparation.

Table 1. Analysis of HNE-modified peptides derived from α- and β-spectrin by MALDI-TOF MS.

Tryptic peptides derived from α- and β-spectrin were analyzed for Michael-type (Michael) and Schiff base (Schiff) HNE adducts by MALDI-TOF MS. The amino acid residues, sequences, and theoretical and observed masses are shown for peptides deduced to contain HNE adduct(s) by at least two independent analyses (peptides 1-16 and 1-18 for α- and β-spectrin, respectively). Localization of each peptide in the spectrin repeats is also indicated.

Spectrin	Peptide number	Spectrin repeats	Amino acid residues	Sequence	Mass		Numbers of HNE adducts†	
					Theoretical	Observed	Michael	Schiff
α-Spectrin	1*	3-4	257-271	QKALSNAANLQRFKR	1743.99	2057.18	2	0
	2	4	295-307	DLVASEGLFHSHK	1438.72	1597.85	1	0
	3*	4	312-326	NLAVMSDKVKELCAK	1647.87	2117.21	3	0
	4	4	322-329	ELCAKAEK	890.45	1207.65	2	0
	5*	5	412-416	HQQHK	676.34	989.56	2	0
	6	7	569-575	EKAATRR	830.47	989.56	1	0
	7*	7	596-601	NWINKK	801.45	958.54	1	0
	8*	13	1225-1230	HEGFER	773.35	930.49	1	0
	9*	13-14	1282-1290	KESLNEAQK	1045.54	1202.70	1	0
	10	13-14	1283-1299	ESLNEAQKFYLFLSKAR	2043.08	2202.15	1	0
	11*	16	1586-1594	EHVVDHLLER	1233.59	1546.89	2	0
	12	17	1648-1659	KHQLLEREMLAR	1522.84	1663.83	0	1
	13	18	1744-1756	DLQGVQNLLKKHK	1519.88	1818.94	1	1
	14*	20	2016-2027	WEQLLEASAVHR	1437.74	1594.95	1	0
	15	21	2133-2141	HLSDIIEER	1110.57	1269.71	1	0
	16*	EF1	2281-2293	HFDENLTGRLTHK	1566.79	1723.98	1	0
β-Spectrin	1	Nt	45-52	IKALADER	914.52	1055.56	0	1
	2*	Nt	75-86	ITDLYKDLRDGR	1463.77	1620.88	1	0
	3*	Nt	110-118	IHCLENVDK	1069.52	1382.65	2	0
	4*	Nt	110-124	IHCLENVDKALQFLK	1769.95	2239.24	3	0
	5	Nt	110-127	IHCLENVDKALQFLKEQR	2183.15	2622.46	1	2
	6	Nt	227-243	DSNARHNLEHAFNVAER	1978.94	2138.08	1	0
	7*	1	293-302	VIDHAIETEK	1153.60	1310.70	1	0
	8*	2	491-498	ENYHDQKR	1088.50	1401.74	2	0

9	3	570-593	HKLMEADIAIQGDKVKAITAATLK	2564.44	2705.48	0	1
10*	4	631-641	TQLEQSKRLWK	1415.79	1572.79	1	0
11*	7	956-975	VHTLCVDCEETSKWITDKTK	2335.12	2705.48	2	0
12	7	974-996	TKVVESTKDLGRDLAGIIAIQRK	2510.45	2827.62	2	0
13	9	1161-1175	SHTLAQCLGFQEFQK	1735.84	1894.98	1	0
14	11	1404-1420	SDDPRKDLTSVNRMLAK	1945.00	2104.03	1	0
15	11	1417-1431	MLAKLKRVEDQVNVR	1798.02	1938.91	0	1
16	14	1671-1684	HYAGLKDVAEERKR	1670.89	1830.01	1	0
17	14	1677-1696	DVAEERKRKLENMYHLFQLK	2546.34	2705.48	1	0
18*	17	1991-2004	RKEMNEKWEARWER	1946.95	2260.14	2	0

*Obtained for α- and β-spectrin without reduction. Other HNE-peptides were detected for polypeptides reduced with $NaBH_4$ prior to tryptic digestion.

†Numbers of deduced HNE-amino acid adducts in each peptide.

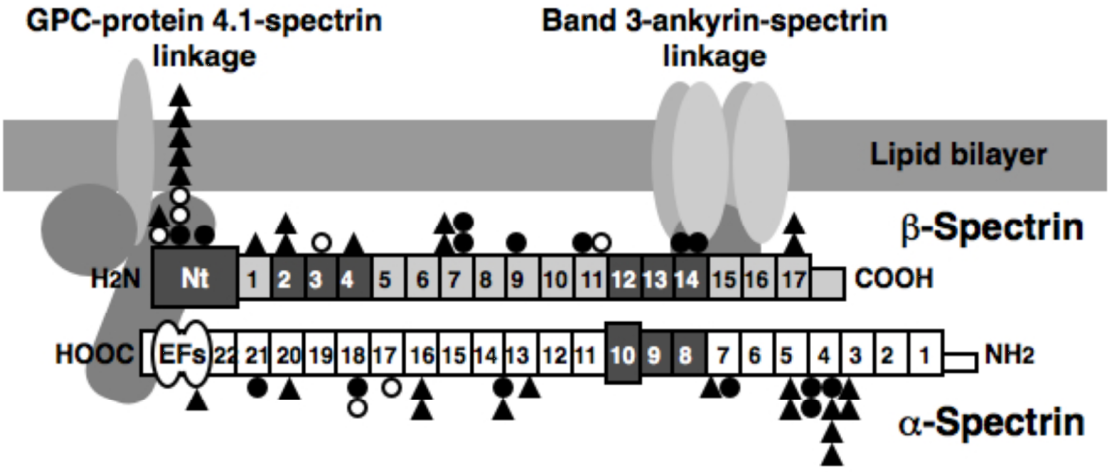

Figure 3. Schematic illustration of HNE-amino acid adduct positions in α- and β-spectrin deduced from MALD-TOF MS analysis.

Positions of HNE-amino acid adducts found in α- and β-spectrin by MALDI-TOF MS analysis (Table 1) are summarized and schematically presented. Closed and open circles indicate Michael-type and Schiff base adducts, respectively, for spectrins reduced with $NaBH_4$ prior to MS analysis. Closed triangles indicate Michael adducts deduced for spectrins without reduction. Illustrations for spectrin and phosphatidylserine-binding repeats are according to previous studies (Mohandas and Gallagher, 2008; An *et al*., 2004). Interactions between spectrin and membrane proteins through glycophorin C-protein 4.1-spectrin and band 3-ankyrin-spectrin linkages are also shown.

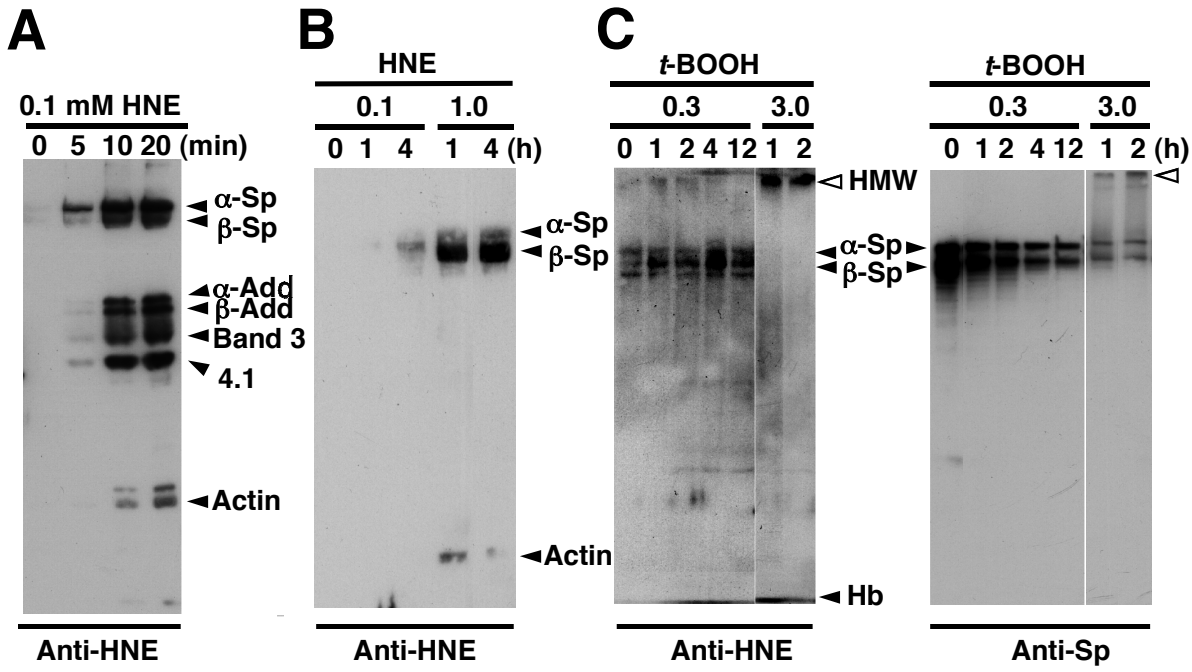

Figure 4. HNE-spectrin adduct formation in RBC ghosts and intact red cells exposed to HNE.

A. Human RBC ghosts were suspended in PBS containing 0.1 mM HNE and placed on ice for 10 minutes then incubated at 37ºC for the indicated periods and analyzed for HNE-protein adduct formation by immunoblotting (5 μg/lane) with the anti-HNE antibody. **B.** Human RBCs were incubated at 37ºC in the presence of 0.1 or 1.0 mM HNE for 0, 1 or 4 hours. RBC membrane ghosts were prepared and analyzed by immunoblotting (5 μg/lane). Immunoblotting membranes were exposed to films for 3-5 seconds. **C.** RBCs were incubated at 37ºC for 0-12 hours with 0.3 or 3.0 mM *t*-BOOH. After a brief wash, packed RBCs were directly solubilized in an equivalent volume of 2× SDS-PAGE sample buffer, and were subjected to immunoblotting to detect HNE-protein adducts (*Anti-HNE*) and spectrin (*Anti-Sp*). Closed arrowheads indicate α- and β-spectrin (*α-Sp* and *β-Sp*) and some major proteins in the red cell membranes, including α- and β-adducin (*α-Add* and *β-Add*), band 3, protein 4.1, actin, and hemoglobin (*Hb*). Open arrowheads indicate high molecular weight aggregates (*HMW*).

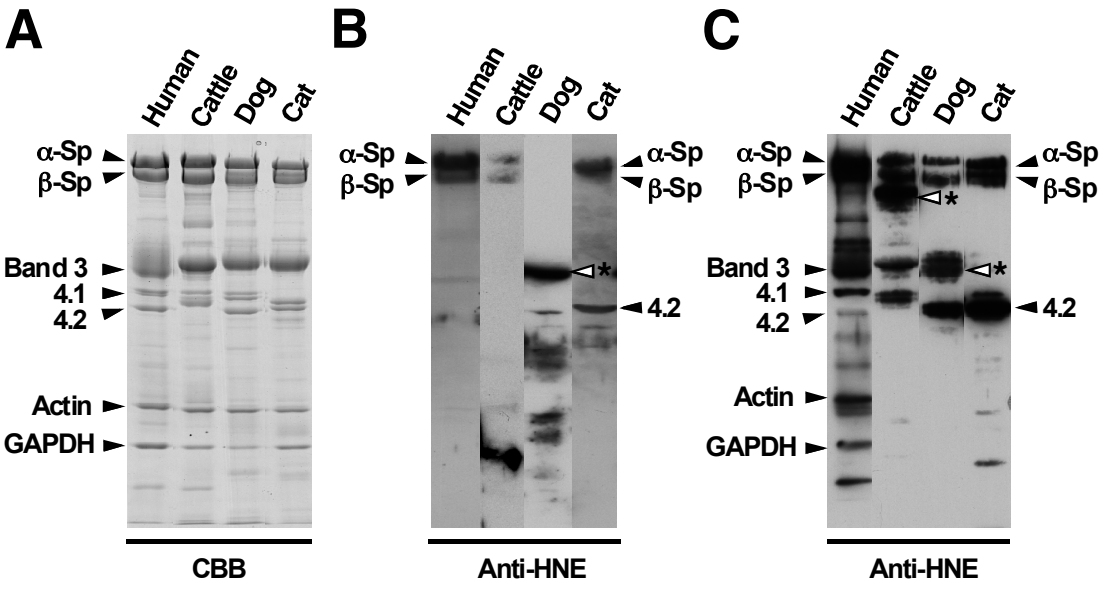

Figure 5. HNE adduct formation in red cell membranes from several animal species.

A. Membrane proteins (8 μg/lane) from human (*Human*), bovine (*Cattle*), canine (*Dog*), and feline (*Cat*) red cells were separated by SDS-PAGE followed by Coomassie brilliant blue staining (*CBB*). **B** and **C.** HNE-protein adduct formation was analyzed by immunoblotting using the anti-HNE adduct (*Anti-HNE*) antibody. In immunoblotting, the membranes were exposed to the films for 1 minute. In *C*, red cell ghosts were suspended in PBS containing 0.1 mM HNE and placed on ice for 10 minutes then incubated at 37ºC for 1 hour and analyzed for HNE-protein adduct formation by immunoblotting (5 μg/lane). Immunoblotting membranes were exposed to films for 3-5 seconds. The migrating positions of the major membrane proteins, including α- and β-spectrin (*α-Sp* and *β-Sp*, respectively), are indicated. Arrowheads with asterisks indicate unidentified polypeptides of 200 kDa and 95 kDa in bovine and canine membranes, respectively.

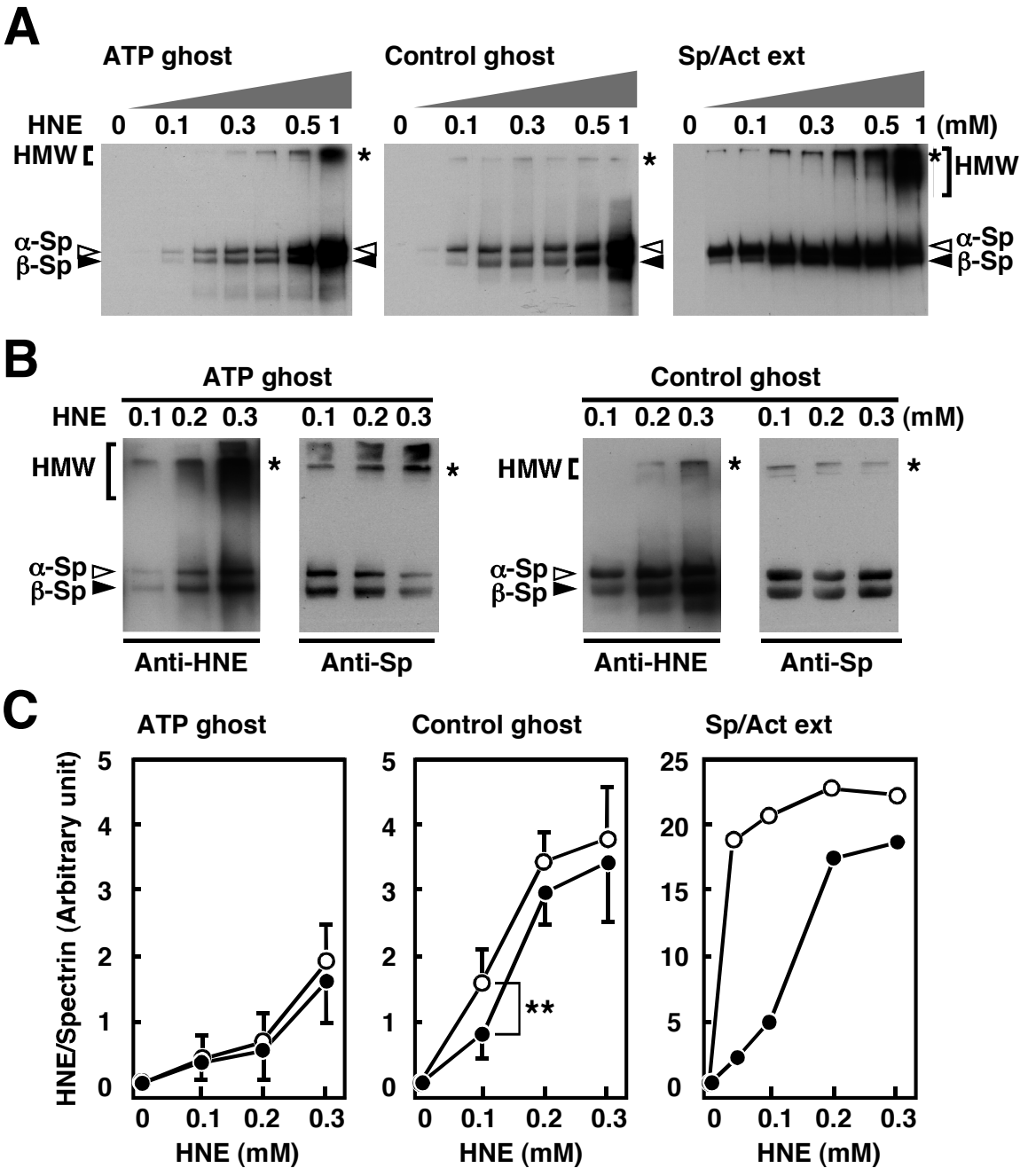

Figure 6. HNE-spectrin adduct formation in MgATP ghosts and control ghosts exposed to HNE.

(continued on the following page)

Figure 6. HNE-spectrin adduct formation in MgATP ghosts and control ghosts exposed to HNE.

A. Human red cell ghosts were prepared in hypotonic buffer (5 mM Tris/Cl. pH 7.4, 5 mM KCl, 1 mM $MgCl_2$) with or without 0.6 mM MgATP (*MgATP ghost* and *Control ghost*, respectively) and were diluted in the same buffer to contain 0.1 mM MgATP when present. These ghosts were incubated at 37ºC and 1 mg protein/ml for 1 hour with 0, 0.05, 0.1, 0.2, 0.3, 0.4, 0.5, or 1.0 mM HNE. After rapid centrifugation, the membrane proteins (1 μg/lane) were analyzed for HNE-protein adducts by immunoblotting. Crude extracts containing spectrin and actin (*Sp/Act ext*, 0.3 mg protein/ml) were also incubated with HNE and processed to detect HNE-protein adducts (0.3 μg/lane). **B.** Typical immunoblots similar to those shown in *A*, with longer exposure time for HNE-protein adducts (*Anti-HNE*), and the corresponding immunoblots for spectrin (*Anti-Sp*). In *A* and *B*, α- and β-spectrin (*α-Sp* and *β-Sp*) and high molecular weight species (*HMW*) are indicated. Asterisks mark the top of the separating gel. Immunoblot membranes were exposed to films for 3 seconds and 10 seconds in *A* and *B*, respectively. **C.** Contents of HNE-modified α-spectrin (open circles) and β-spectrin (closed circles) shown in *B* were quantified by densitometric scanning, normalized by the corresponding spectrin, and shown as the relative abundance of the HNE-spectrin (*HNE/Spectrin*). Data are the means ± S.D. (n = 3). $^{**}P < 0.01$. The third panel displays data for the crude extracts of spectrin/actin obtained from immunoblots shown in *A*, and the corresponding immunoblots for spectrin (*Sp/Act ext*, n = 2).

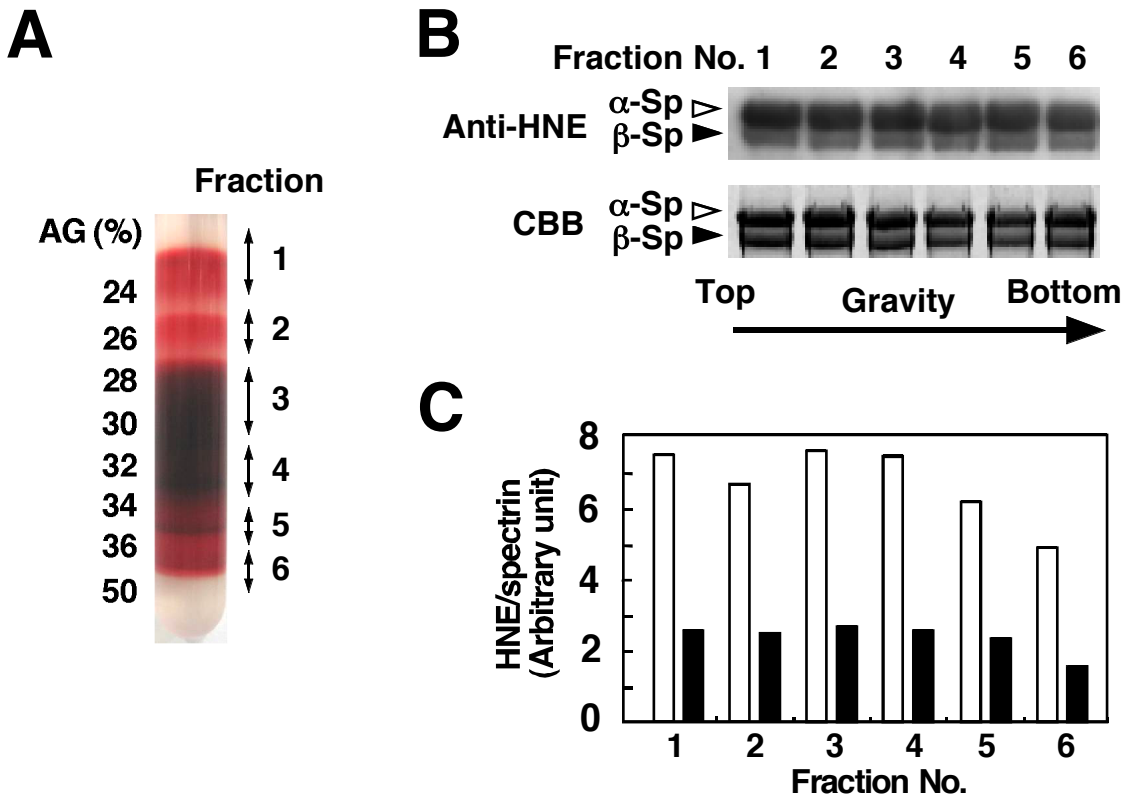

Figure 7. HNE-spectrin adduct contents in density-separated human red cells.
A. Human red cells were separated into fractions 1 to 6 by centrifugation on an arabinogalactan (*AG*) density gradient (Tiffert *et al*., 2005). **B.** Fractions were examined for their HNE-spectrin and whole spectrin contents as described above by immunoblotting (*Anti-HNE*, 8 μg/lane, exposed for 1 minute) and Coomassie brilliant blue staining (*CBB*, 8 μg/lane), respectively. **C.** Contents of HNE-modified α-spectrin (hatched columns) and β-spectrin (unhatched columns) shown in *B* were quantified by densitometric scanning, normalized by the corresponding spectrin, and shown as the relative abundance of the HNE-spectrin (*HNE/Spectrin*). Data represent a typical result from several independent experiments.

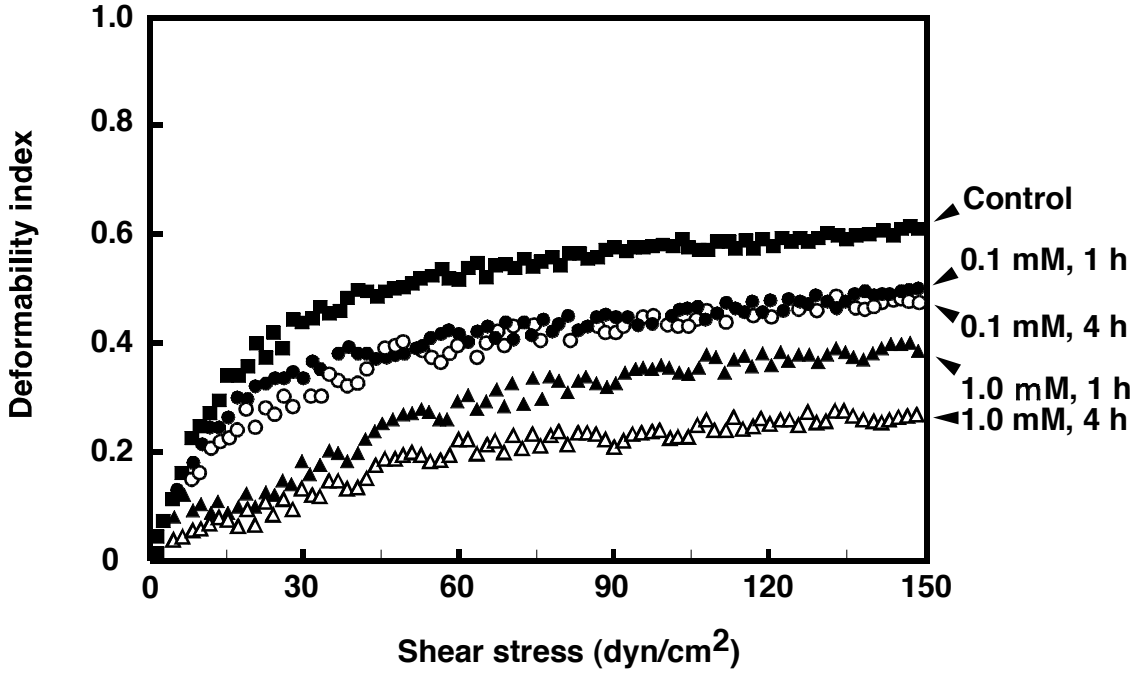

Figure 8. Reduction in deformability of human red cells incubated with HNE.
Human red cells were incubated at 37ºC in the presence (*0.1 mM* or *1.0 mM*) or absence (*Control*) of HNE for 1 or 4 hours (*1 h* or *4 h*), suspended in the PVP solution, and examined for their deformability under an increasing shear stress (0-150 dynes/cm^2) in the ektacytometer. Symbols indicate as follows: *closed square*, control red cells; *closed* and *open circles*, red cells incubated with 0.1 mM HNE for 1 and 4 hours, respectively; *closed* and *open triangles*, red cells incubated with 1.0 mM HNE for 1 and 4 hours, respectively.

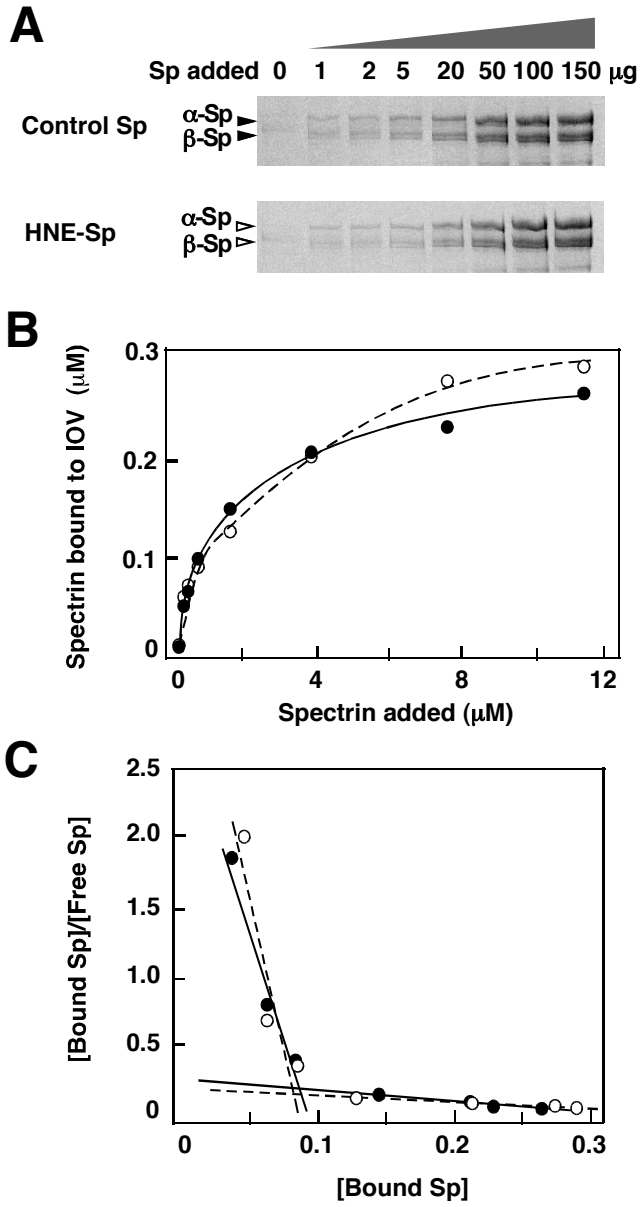

Figure 9. Effect of HNE on binding of spectrin to the IOVs.

A. Spectrin dimers (*Sp*) were extracted from human red cell membranes and incubated at 37ºC in the presence (*HNE-Sp*) or absence (*Control Sp*) of 0.1 mM HNE for 20 minutes. These spectrins (0-150 μg) were incubated with IOVs (10 μg protein) on ice for 90 minutes, then spectrins bound to the IOVs were separated from unbound molecules by centrifugation and analyzed by SDS-PAGE with Coomassie brilliant blue staining. The α- and β-spectrin (*α-Sp* and *β-Sp*) are indicated. **B.** Data are plotted for the amounts of spectrin obtained in IOV pellets are plotted in a function of spectrin added to the reactions. **C.** Scatchard plot for experimental data in *B* shows that the spectrin-IOV interactions observed consist of two linear components with different Kd values. In *B* and *C*, data for control spectrin and HNE-modified spectrin are indicated by closed circles with solid line and open circles with broken line, respectively.

Discussion

Physiological and pathological roles of HNE modification of spectrin

Various diseases involve proteins modified by HNE and protein cross-linking through HNE adducts contributes to disease pathogenecities (Montine *et al*., 1996; Murray *et al*., 2007; Stewart *et al*., 2007; Kokubo *et al*., 2008). Here, we showed that spectrins are the primary targets of HNE, and that HNE-modified spectrins generate irreversibly cross-linked aggregates in human RBCs. Since HNE accumulates in RBCs in circulation (Ando *et al*., 1995), the extensive modification of spectrins by HNE may occur in peripheral blood RBCs under physiological and pathological conditions, leading to RBC senescence or accelerated destruction of RBCs (Fig. 10).

The relative abundance of HNE-spectrin adducts was higher in control ghosts than in MgATP ghosts. MgATP helps maintain the asymmetric distribution of PS through the action of MgATP-dependent phospholipid translocase. Interactions between aminophospholipids and skeletal proteins modulate the human RBC membrane mechanical stability (Manno *et al*., 2002). The spectrin-actin network is thus tightly associated with the lipid bilayer through the direct binding of spectrin with PS in the presence of MgATP (Manno *et al*., 2002) as well as through protein-protein interactions (Mohandas and Gallagher, 2008). Therefore, in the absence or under reduced concentrations of MgATP, greater HNE adduct formation may occur in spectrins that are dissociated from the lipid bilayer and have increased susceptibility to the amphiphilic HNE. Then, local aggregation of HNE-modified spectrins is inevitable, since these spectrins contain Cys-, His-, and Lys-Michael adducts and Schiff bases on the Lys

residues, that are required for intra- or intermolecular cross-linking (Esterbauer *et al*., 1991; Uchida *et al*., 1993; Petersen and Doorn, 2004; Murray *et al,* 2007; Stewart *et al*., 2007). Local spectrin aggregation may free the lipid bilayer from underlying spectrin-actin skeletons, possibly leading to membrane surface area loss by extrusion, which occurs in RBCs under oxidative conditions (Snyder *et al*., 1998; Wagner *et al*., 1987) and various RBC membrane disorders (Tse and Lux, 2001; Mohandas and Gallagher, 2008; Perotta *et al*., 2008) (Fig. 10). Thus, in addition to modulating RBC membrane mechanical properties, the spectrin-membrane lipid interactions may have an obligatory role in preventing skeletal proteins from excessive HNE adduct formation.

In contrast to the observations under ATP-free conditions described above, in which HNE modifications preferentially occurred in α-spectrin (Figs. 4 and 6), the intensities of β-spectrin HNE adducts were comparable to those of α-spectrin in HNE-exposed MgATP ghosts (Fig. 6). Furthermore, β-spectrin was the principal target of HNE when intact RBCs were exposed to HNE or *t*-BOOH (Fig. 4). Spectrin reportedly associates directly with PS (Cohen *et al*., 1986; Manno *et al*., 2002) in several distinct segments involving the N-terminal actin-binding domain, triple helical structural repeats 2-4 and 12-14 of β-spectrin, and repeats 8-10 of α-spectrin (An *et al*., 2004). Thus, under physiological conditions, HNE adduction occurs preferentially in membrane-associated β-spectrin at the interface of the skeletal protein and the inner leaflet of the membrane lipid bilayer. Intrinsic HNE is generated in the lipid bilayer by fatty acid peroxidation; extrinsic HNE reaches the inner leaflet presumably by diffusion through the lipid bilayer (Uchida, 2003). These assumptions are consistent with the presence of HNE adducts in the N-terminal regions of β-spectrin, including repeats 2-4 (Fig.

3). Moreover, selective HNE-spectrin formation and protection of other membrane proteins from HNE addition probably involve HNE elimination by cellular glutathione. Glutathione readily reacts with HNE via Michael addition spontaneously or enzymatically to form glutathione-HNE conjugate and much of aqueous HNE in a cell is bound to glutathione (Petersen and Doorn, 2004).

Interestingly, in the presence of MgATP, the HNE-modified spectrins tended to be cross-linked and aggregated (Fig. 6). HNE reportedly modifies the three His residues of amyloid β protein (Aβ). These HNE-modified Aβ molecules have an increased affinity for membrane lipids and possess a conformation similar to that of mature amyloid fibrils (Murray *et al*., 2007; Liu *et al*., 2008). The observed enrichment of HNE-His adducts (Fig. 2 and Table 1) suggests that the propensity of HNE-modified spectrin to form aggregates may involve mechanisms similar to those found for Aβ. Thus, the closer to the physiological environment the RBC membrane is, the more readily membrane damage through spectrin aggregation can occur. Consequently, restricted membrane surface area loss would occur with much less severity compared to pathological conditions described above. This mechanism, involving preferential β-spectrin HNE-modification and aggregate formation, may provide significant protection against excessive lipid peroxidation product accumulation during RBC aging. The slightly decreased contents of HNE-spectrin adducts in the most dense population (Fig. 7), which displayed reduced membrane surface area/volume ratios possibly represent the gradual accumulation followed by the loss of aggregated HNE-modified proteins and membrane lipids during RBC aging (Fig. 10). This mechanism also gives an explanation for the difference between ghosts from intact RBCs (Fig. 2) and ghosts from HNE-exposed RBCs

(Fig. 4) in HNE modification patterns of α- and β-spectrin. HNE modification and consequent aggregate formation would be expected for spectrin family members expressed at the cytoplasmic plasma membrane surface of most metazoan cells (Bennett and Healy, 2008).

HNE-spectrin aggregation in the presence of ATP may also involve interactions with hemoglobin. The MgATP ghost contained more residual hemoglobin (~12% of the total membrane proteins) than the control ghost (< 3% of the total membrane proteins). Retained hemoglobin can augment irreversible aggregate formation, possibly by cross-linking spectrin, as previously shown in human red blood exposed to hydrogen peroxide (Snyder *et al*., 1985).

Characteristics of HNE modification of spectrin and its effects on the protein function

One of the most notable findings of the present study is that human RBCs exposed to HNE exhibited marked reduction in their deformability (Fig. 8). Since spectrin was the major target of HNE in the RBC membranes under the condition employed (Figs. 4 and 8), this implies that HNE modification caused structural and/or functional changes of spectrin, leading to reduced mechanical properties of the RBC membrane. The possible changes in spectrin skeleton in RBCs treated with HNE appear to differ from those reported for the RBCs exposed to oxidants to generate spectrin-hemoglobin cross-linking (Snyder *et al*., 1985; Wagner *et al*., 1987). In these RBCs, lipid peroxidation, though present, was not necessary for the formation of spectrin-hemoglobin aggregates and the various cellular changes (Snyder *et al*., 1985). As discussed above, therefore, surface area loss due to aggregate formation of HNE-spectrin might be a cause for the decreased deformability of RBCs incubated with HNE.

The other possibility involves a slight increase in interactions between spectrin and its binding proteins in the membrane such as protein 4.1R and/or ankyrin-band 3 complex (Tse and Lux, 2001; Mohandas and Gallagher, 2008). The stoichiometry of binding of control spectrin heterodimers to the IOVs with K_d of 0.8 μM observed (Fig. 9) is comparable with that reported for binding of protein 4.1R and ankyrin to spectrin in the 10^{-7} M range (Tyler *et al*., 1980). The increased affinity of HNE-modified spectrin with K_d of 0.4 μM likely represent that structural changes caused by HNE adduction can modulate the membrane binding stoichiometry of spectrin through the protein-protein association. On the other hand, there was no significant change in the low affinity component of the spectrin-IOV binding that appears to represent a direct association of spectrin to the membrane lipids (PS) with $K_d = 10^{-5} \sim 10^{-6}$ M range (An *et al*., 2004). This is contrary to the assumption discussed above, i.e., an increased affinity of HNE-spectrin to the membrane lipids. This discrepancy may be attributed to the lack of asymmetric distribution of PS in the IOVs due to the absence of MgATP in the reaction. Measurement of deformability of resealed ghosts would provide some clues to these issues.

HNE adduct formation was shown to be a posttranslational modification of spectrin polypeptides, with several major, distinct target sites susceptible to HNE (Fig. 3). This posttranslational event seemingly can occur soon after spectrin synthesis, since HNE-spectrin adducts were found in all fractions, including the lightest/youngest fraction, of density-separated red cells (Fig. 7). We also observed that an anti-HNE antibody reacted with bacterial recombinant polypeptides of the N-terminal domain and the adjacent triple helical structural repeats 2-4 of β-spectrin (An *et al*., 2004), and that some tryptic peptides of these

recombinants showed mass shifts indicative of Michael-type adducts (data not shown). For example, the peptide IHCLENVDK (amino acid residues 110-118, $[M + H]^+$ with an *m/z* of 1,382.6) exhibited a mass shift of 312 *m/z* due to two Michael adducts at the His and Cys residues, as demonstrated for the native RBC spectrins. There should be some structural changes subsequent to HNE adductions, particularly in the N-terminal β-spectrin region. It should be ascertained whether such structural changes affect or modulate spectrin function, since this region and the α-spectrin C-terminus play key roles in αβ heterodimer formation (Speicher *et al*., 1992; Begg *et al*., 2000) and actin and protein 4.1 binding (Tse and Lux, 2001; An *et al*., 2005; Zhu *et al*., 2007).

In conclusion, this study demonstrates that HNE-spectrin adducts spontaneously form at the interface of membrane skeletal proteins and the inner lipid bilayer leaflet in human RBCs. Furthermore, our data suggests that HNE-spectrin aggregates may accumulate in the RBC, followed by their extrusion with membrane lipids from RBCs. This process may be involved in the physiological and pathological destruction of RBCs.

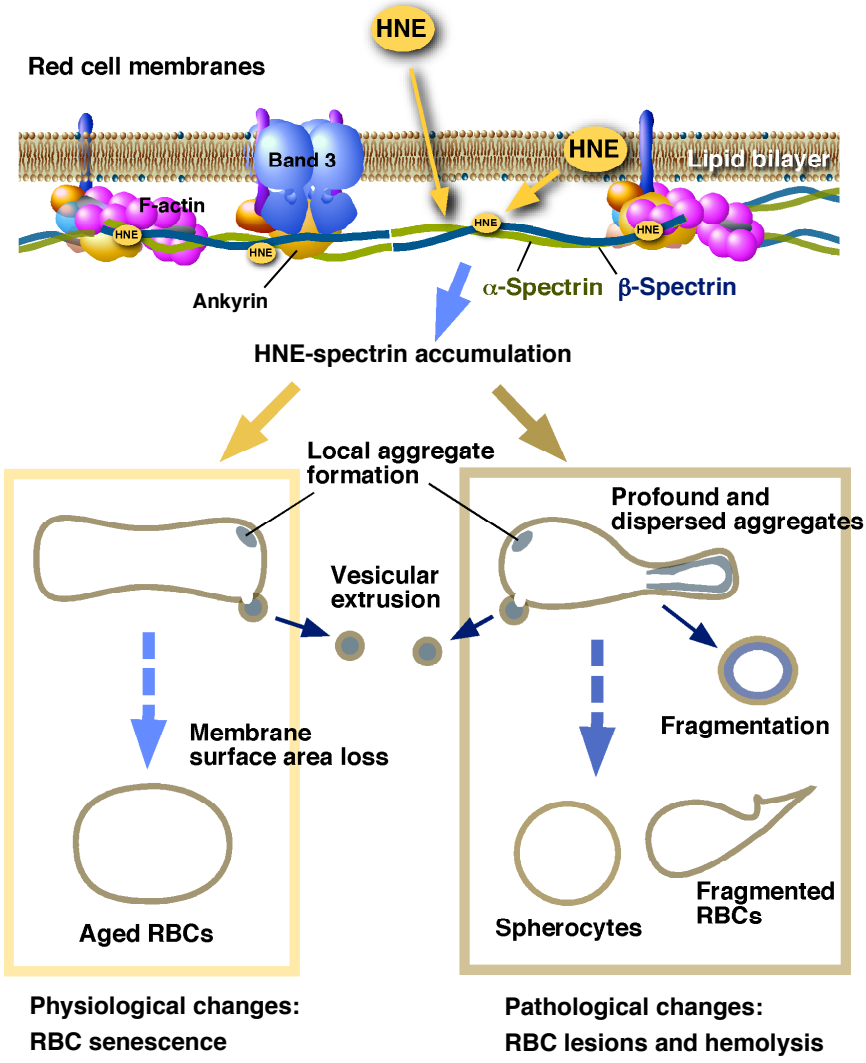

Figure 10. Schematic illustration for HNE-spectrin adduct formation and its implications in physiological and pathological changes of RBCs.

Both intrinsic HNE generated in the membrane through lipid peroxidation in RBCs and extrinsic HNE penetrated through the lipid bilayer can react with spectrin to form HNE-spectrin adducts. Accumulated HNE-modified spectrin, depending on the extent to which levels accumulation occurs, may generate local or large and dispersed aggregates. Vesicular extrusion of the local aggregates consequently cause membrane surface area loss in RBCs under physiological condition, resulting in production of aged and sphere RBCs. By contrast, under some pathological conditions generating HNE at profound levels, aggregates formed aberrantly and extensively at the cytoplasmic surface of RBC membranes would cause fragmentation of RBCs, resulting in hemolysis.

References

An, X., Debnath, G., Guo, X., Liu, S., Lux, S. E., Baines, A., Gratzer, W. and Mohandas, N. (2005) Identification and functional characterization of protein 4.1R and actin-binding sites in erythrocyte spectrin: regulation of the interactions by phosphatidylinositol-4,5-bisphosphate. *Biochemistry* **44**: 10681-10688.

An, X., Guo, X., Sum, H., Morrow, J., Gratzer, W. and Mohandas, N. (2004) Phosphatidylserine binding sites in erythroid spectrin: location and implications for membrane stability. *Biochemistry* **43**: 310-315.

Ando, K., Beppu, M. and Kitagawa, K. (1995) Evidence for accumulation of lipid hydroperoxides during the aging of human red blood cells in the circulation. *Biol Pharmacol. Bull.* **18**: 659-663.

Becker, P. S., Cohen, C. M, and Lux, S. E. (1986) The effect of mild diamide oxidation on the structure and function of human erythrocyte spectrin. *J. Biol. Chem.* **261**: 4620-4628.

Begg, G. E., Harper, S. L., Morris, M. B. and Speicher, D. W. (2000) Initiation of spectrin dimerization involves complementary electrostatic interactions between paired triple-helical bundles. *J. Biol. Chem.* **275**: 3279-3287.

Bennett, V. and Healy, J. (2008) Organizing the fluid membrane bilayer: diseases linked to spectrin and ankyrin. *Trends Mol. Med.* **14**: 28-36.

Chasis, J. A. and Mohandas, N. (1986) Erythrocyte membrane deformability and stability: two distinct membrane properties that are independently regulated by skeletal protein associations. *J. Cell Biol.* **103**: 343-350.

Cohen, A. M., Liu, S.-C., Derick, L. H. and Palek, J. (1986) Ultrastructural studies of the interaction of spectrin with phosphatidylserine liposomes. *Blood* **68**: 920-926.

Esterbauer, H., Schauer, R. J. and Zollner, H. (1991) Chemistry and biochemistry of 4-hydroxynonenal, malondialdehyde and related aldehydes. *Free Rad. Biol. Med.* **11**: 81-128.

Fenaille, F., Guy, P. A. and Tabet, J. C. (2003) Study of protein modified by 4-hydroxy-2-nonenal and other short chain aldehydes analyzed by electrospray ionization tandem mass spectrometry. *J. Am. Soc. Mass Spectrom.* **14**: 215-226.

Ito, D., Koshino, I., Arashiki, N., Adachi, H., Tomihari, M., Tamahara, S., Kurogi, K., Amano, T., Ono, K. and Inaba, M. (2006) Ubiquitylation-independent ER-associated degradation of an AE1 mutant associated with dominant hereditary spherocytosis in cattle. *J. Cell Sci.* **119**: 3602-3612.

Inaba, M. and Maede, Y. (1988) A new major transmembrane glycoprotein, gp155, in goat erythrocytes. Isolation and characterization of its association to cytoskeleton through binding with band 3-ankyrin complex. *J. Biol. Chem.* **263**: 17763-17771.

Inaba, M. and Maede, Y. (1989) O-*N*-Acetyl-D-glucosamine moiety on discrete peptide of multiple protein 4.1 isoforms regulated by alternative pathways. *J. Biol. Chem.* **264**: 18149-18155.

Inaba, M., Gupta, K. C., Kuwabara, M., Takahashi, T., Benz, E. J. Jr, and Maede, Y. (1992) Deamidation of human erythrocyte protein 4.1: possible role in aging. *Blood* **79**: 3355-3361.

Inaba, M., Yawata, A., Koshino, I., Sato, K., Takeuchi, M., Takakuwa, Y., Manno, S.. Kanzaki, A., Sakai, J., Ban, A., Ono, K. and Maede, Y. (1996) Defective anion transport and marked spherocytosis with membrane instability caused by hereditary total deficiency of red cell band 3 in cattle due to a nonsense mutation. *J. Clin. Invest.* **97**: 1804-1817.

Jain, S. K. (1988) Evidence for membrane lipid peroxidation during the in vivo aging of human erythrocytes. *Biochim. Biophys. Acta* **937**: 205-210.

Kokubo, J., Nagatani, N., Hiroki, K., Kuroiwa, K., Watanabe, N. and Arai, T. (2008) Mechanism of destruction of microtubule structures by 4-hydroxy-2-nonenal. *Cell Struct. Funct.* **33**: 51-59.

Lauderback, C. M., Hackett, J. M., Huang, F. F., Keller, J. N., Szweda, L. I., Markesbery, W. R. and Butterfield, D. A. (2001) The glial glutamate transporter, GLT-1, is oxidatively modified by 4-hydroxy-2-nonenal in the Alzheimer's disease brain: the role of Aβ1-42. *J. Neurosci.* **78**: 413-416.

Liu, L., Komatsu, H., Murray, I. V. J. and Axelsen, P. H. (2008) Promotion of amyloid β protein misfolding and fibrillogenesis by a lipid oxidation product. *J. Mol. Biol.* **377**, 1236-1250.

Liu, Z., Minkler, P. E. and Sayre, L. M. (2003) Mass spectroscopic characterization of protein modification by 4-hydroxy-2-(*E*)-nonenal and 4-oxo-2-(*E*)-nonenal. *Chem. Res. Toxicol.* **16**, 901-911.

Low, P. S., Willardson, B. M., Mohandas, N., Rossi, M. and Shohet, S. (1991) Contribution of the band 3-ankyrin interaction to erythrocyte membrane stability. *Blood* **77**: 1581-1586.

Manno, S., Takakuwa, Y. and Mohandas, N. (2002) Identification of a functional role for lipid asymmetry in biological membranes: phosphatidylserine-skeletal protein interactions modulate membrane stability. *Proc. Natl. Acad. Sci. U.S.A.* **99**: 1943-1948.

Mohandas, N. and Gallagher, P. G. (2008) Red cell membrane: past, present, and future. *Blood* **112**: 3939-3948.

Montine, T. J., Amarnath, V., Martin, M. E., Strittmatter, W. J. and Graham, D. G. (1996) E-4-Hydroxy-2-nonenal is cytotoxic and cross-links cytoskeletal proteins in P19 neuroglial cultures. *Am. J. Pathol.* **148**: 89-93

Murray, I. V. J., Liu, L., Komatsu, H., Uryu, K., Xiao, G., Lawson, J. A. and Axelsen, P. H. (2007) Membrane-mediated amyloidogenesis and the promotion of oxidative lipid damage by amyloid β proteins. *J. Biol. Chem.* **282**: 9335-0345.

Perrotta, S,, Gallagher, P. G. and Mohandas, N. (2008) Hereditary spherocytosis. *Lancet* **372**: 1411-1426.

Petersen, D. R. and Doorn, J. A. (2004) Reactions of 4-hydroxynonenal with proteins and cellular targets. *Free Rad. Biol. Med.* **37**: 937-945.

Schneider, C., Tallman, K. A., Porter, N. A. and Brash, A. R. (2001) Two distinct pathways of formation of 4-hydroxynonenal. Mechanisms of nonenzymatic transformation of the 9- and 13-hydroperoxides of linoleic acid to 4-hydroxyalkenals. *J. Biol. Chem.* **276**: 20831-20838.

Speicher, D. W., Weglarz, L. and SeSilva, T. M. (1992) Properties of human red cell spectrin

heterodimer (side-to-side) assembly and identification of an essential nucleation site. *J. Biol. Chem.* **267**: 14775-14782.

Stewart, B. J., Doorn, J. A. and Petersen, D. R. (2007) Residue-specific adduction of tubulin by 4-hydroxynonenal and 4-oxononenal causes cross-linking and inhibits polymerization. *Chem. Res. Toxicol.* **20**: 1111-1119.

Snyder, L. M., Fortier, N. L., Trainer, J., Jacobs, J., Leb, L., Lubin, B., Chiu, D., Shohet, S. and Mohandas, N. (1985) Effect of hydrogen peroxide exposure on normal human erythrocyte deformability, morphology, surface characteristics, and spectrin-hemoglobin cross-linking. *J. Clin. Invest.* **76**: 1971-1977.

Tiffert, T., Lew, V. L., Ginsburg, H., Krugliak, M., Croisille, L. and Mohandas, N. (2005) The hydration state of human red blood cells and their susceptibility to invasion by *Plasmodium falciparum*. *Blood* **105**: 4853-4860.

Tse, W. T. and Lux, S. E. (2001) Hereditary spherocytosis and hereditary elliptocytosis. In: Scriver CR, Beaudet AL, Sly WS, Valle DV, eds. The Metabolic & Molecular Bases of Inherited Disease (8th edition). New York, NY: McGraw-Hill: 4665-4727.

Tyler, J. M., Reinhardt, B. N. and Branton, D. (1980) Association of erythrocyte membrane proteins. Binding of purified bands 2.1 and 4.1 to spectrin. *J. Biol. Chem.* **255**: 7034-7039.

Uchida, K. (2003) Review. 4-Hydroxy-2-nonenal: a product and mediator of oxidative stress. *Prog. Lipid Res.* **42**: 318-343.

Uchida, K., Hasui, Y. and Osawa, T. (1997) Covalent attachment of 4-hydroxy-2-nonenal to erythrocyte proteins. *J. Biochem.* **122**: 1246-1251.

Uchida, K., and Stadtman, E. R. (1993) Covalent attachment of 4-hydroxynonenal to glyceraldehyde-3-phosphate dehydrogenase. A possible involvement of intra- and intermolecular cross-linking reaction. *J. Biol. Chem.* **268**: 6388-6393.

Wagner, G. M., Chiu, D. T.-Y., Qju, J. H., Heath, R. H. and Lubin, B. H. (1987) Spectrin oxidation correlates with membrane vesiculation in stored RBCs. *Blood* **69**: 1777-1781.

Yang, Y., Sharma, R., Sharma, A., Awasthi, S and Awasthi, Y. C. (2003) Lipid peroxidation

and cell cycle signaling: 4-hydroxynonenal, a key molecule in stress mediated signaling. *Acta Biochim. Polon.* **50**: 319-336.

Zhu, Q., Vera, C., Asaro, R. J., Sche, P. and Sung, L. A. (2007) A hybrid model for erythrocyte membrane: a single unit of protein network coupled with lipid bilayer. *Biophys. J.* **93**: 386-400.

Acknowledgments

The author express sincere gratitude to Professor Mutsumi Inaba (Laboratory of Molecular Medicine, Graduate School of Veterinary Medicine, Hokkaido University) for his excellent supervision and encouragements throughout this work.

I would like to express my great thanks to Professor Yuichi Takakuwa and Associate Professor Sumie Manno (Department of Biochemistry, Tokyo Women's Medical University) for helpful discussions and technical support, Professor Osamu Inanami (Laboratory of Radiation Biology), Associate Professor Akira Terao (Laboratory of Biochemistry), and Associate Professor Kota Sato (Laboratory of Molecular Medicine), all from Graduate School of Veterinary Medicine, Hokkaido University, for their helpful discussion and critical reading of the manuscript. I also express my great thanks to Drs. Yayoi Otsuka, Daisuke Ito, Hiroshi Ohta, Mizuki Tomihari, Tomohiko Komatsu, Hirokazu Adachi and all members of the Laboratory of Molecular Medicine for discussion and technical assistance.

Abstract

Spectrin strengthens the red cell membrane through its direct association with membrane lipids and through protein-protein interactions. Spectrin loss reduces the membrane stability and results in various types of hereditary spherocytosis. However, less is known about acquired spectrin damage. The present study showed that α- and β-spectrin in human red cells are the primary targets of the lipid peroxidation product 4-hydroxy-2-nonenal (HNE) by immunoblotting and mass spectrometry analyses. The level of HNE adducts in spectrin (particularly α-spectrin) and several other membrane proteins was increased following the HNE treatment of red cell membrane ghosts prepared in the absence of MgATP. In contrast, ghost preparation in the presence of MgATP reduced HNE adduct formation, with preferential β-spectrin modification and increased cross-linking of the HNE-modified spectrins. Exposure of intact red cells to HNE resulted in selective HNE-spectrin adduct formation with a similar preponderance of HNE–β-spectrin modifications and marked reduction in the membrane mechanical properties. These findings indicate that HNE adduction occurs preferentially in spectrin at the interface between the skeletal proteins and lipid bilayer in red cells and suggest that HNE-spectrin adduct aggregation results in the extrusion of damaged spectrin and membrane lipids under physiological and disease conditions.

Abstract in Japanese（要　旨）

Modification of Spectrin in Red Cell Membranes by the Lipid Peroxidation Product 4-Hydroxy-2-nonenal Associated with the Changes in Red Cell Membrane Properties

（赤血球膜スペクトリンの脂質過酸化産物 4-ヒドロキシ-2-ノネナールによる分子修飾と赤血球膜物性の変化）

膜脂質の過酸化は、4-hydroxyl-2-nonenal (HNE)をはじめとする種々のアルデヒドやアルケナールを産生する。これらの脂質過酸化産物は、核酸やタンパク質と共有結合して、その構造と機能の障害を生じる。赤血球は、こうした脂質過酸化産物による障害を最も受け得る細胞であり、その老化にともなう HNE の蓄積が知られるが、実際にいかなる分子修飾がどのような影響をもたらすのかは不明である。本研究は、その解明を目的に、主にヒト赤血球膜における HNE 付加タンパク質と修飾部位の同定、ならびに膜物性に対する影響の解析を行った。

まず、抗 HNE 抗体を用いたイムノブロッティングの結果、膜骨格網状構造の主体をなすタンパク質、α-、ならびにβ-スペクトリンに HNE 付加体のシグナルが検出された。赤血球膜ゴーストを HNE と孵置すると、アクチンやバンド３をはじめとする他の主要膜タンパク質に HNE 付加が生じたが、無傷赤血球に HNE を作用させた場合にはスペクトリンにのみ、特にβ-スペクトリンに HNE 付加体の著しい増加が認められ、α-、ならびにβ-スペクトリンが HNE の主たる標的分子であることが明らかになった。飛行時間型質量分析装置を用いた解析から、その修飾部位は、β-スペクトリン分子 N 末端ドメイン(βN)中の Ile^{110}-····-Arg^{127} 配列など、膜脂質と直接に相互作用する領域を中心に複数存在し、Cys、His、ならびに Lys 残基の Michael 付加体として、また Lys 残基では加えて Schiff 塩基付加体として存在すると推定された。一方、ヒト以外の赤血球膜でも、HNE との孵置により HNE-スペクトリンの著増がみられたが、自然付加体の量はヒト赤血球に比べて少なく、また動物種により差異が認められた。これらの知見は、スペクトリン分子と膜脂質との相互作用が HNE 修飾に影響することを示唆するものである。

そこで、赤血球におけるスペクトリン-膜脂質間結合を保つ MgATP の存在／非存在下に膜ゴーストを調製し、これらの HNE 付加を検討した。その結果、MgATP 存在下では、HNE との孵置でスペクトリンの不可溶性凝集体形成が生じ、α鎖よりもβ-スペクトリンの修飾が優位であった。対照的に、MgATP 非存在下では、HNE-α-スペクトリンの生成がβ鎖のそれを上回り、明瞭な凝集はみられなかった。また、比重遠心で分画した赤血球では、予想に反して全ての分画の赤血球でスペクトリンの HNE 修飾がみられ、最下層の老化赤血球では軽度の HNE-スペクトリン減少が認められた。これらの知見は、スペクトリンの膜への組み込み後早期に一定量の HNE 付加が生じることを示すとともに、赤血球の末梢循環過程で限定的な HNE-スペクトリン凝集体の形成と膜小胞としての除去が生じることを示唆している。

さらに、HNE 付加による赤血球膜の機械的特性の変化を知るために、エクタサイトメーターで赤血球の変形能を解析したところ、変形能指数は、HNE の濃度と孵置時間に応じて対照赤血球の値の 40%〜80%に低下した。また、HNE-スペクトリンの赤血球反転小胞への結合定数は対照スペクトリンの約 1/2 とわずかではあるが低下を示した。したがって、一時的な HNE 付加体の増加は、スペクトリン-アクチン膜骨格の変形能を低下させて局所的な膜の断片化を生じ得ると推測され、その一因として赤血球膜との相互作用の強まりが考えられた。

以上のように、本研究の成績は、酸化ストレス下、赤血球内外で生成する HNE が赤血球膜に作用してスペクトリンと共有結合付加体を形成し、スペクトリンの性状と機能を変化させることを通して赤血球膜の変形能を低下させることを明らかにしたものである。これらの知見は赤血球の老化や様々な疾患病態にともなう赤血球膜物性変化に新しい視点を与えるとともに、酸化ストレスが関わる疾患の細胞病態に、膜インターフェースにおける脂質過酸化産物による骨格タンパク質の構造・機能修飾が関わる可能性を示すものである。